METAL FLOW IN THE EXTRUSION OF NON-CIRCULAR SECTIONS

Prof. Dr. A. A. Nasser *, Prof. Dr. M. M. Farag. **
Asst. Prof. S. M. Serag*** and Eng. A. M. Zakzouk ****

ABSTRACT

In production, most extrusion containers are cylinderical, but the extruded section is often other than round. In this paper the flow of pure aluminium was analyzed during the extrusion of non-circular sections from round billets. A modified visioplasticity technique was used to obtain quantitative values of strain rate, strain and flow stress in the deformation zone. Also the extrusion pressure was measured and analysed. The effect of the extrusion ratio and extruded shape geometery on the previous parameters was discussed and was compared with that occured when extruding round shapes. Extrusion experiments were carried out on commercially pure aluminium through square cornered dies and different extrusion ratios. Results showed that The extrusion efficiency was found to be maximum at an extrusion ratio of 14:1. The maximum value of the extrusion efficiency ranged between 45 and 51% depending on the extruded section geometery. The square sections has a more hompgeneous flow than that of rectangular sections.

When extruding a rectangular section the flow in a direction parallel to the length is more homogeneous than that in a direction parallel to the width depending on the width to length ratio. The maximum value of the flow stress, near the die exit, on a plane of symmetry parallel to the width of an extruded rectangular section is more than that found on a plane of symmetry parallel to the length depending on the width to length ratio.

NOMENCLATURE

P_h	: Pressure to overcome homogeneous deformation.	Kg/mm^2
P_r	: Pressure to overcome redundant deformation.	,,
P_f	: Pressure to overcome frictional resistance.	,,
$\bar{\sigma}$	: Flow stress.	,,
A_o	: Initial billet area .	mm^2

* Abdel - Hady Abdel - Bary Nasser , Prof , Dr., Dean of faculty - and chairman of production Engineering & machine design department, Faculty of Engineering and technology, Menoufia university.
** Mahmoud Mohamed Farag , Prof., Dr., Chairman of Materials Engineering Department , American University , Cairo , Egypt .
*** Soad Mohamed Serag , Asst., Prof., Production Engineering & machine design department, Faculty of Engineering & Technology , Menoufia university .
**** Abdel - Aziz Moustafa Zakzouk , B.SC., Demonstrator ,

μ : Coefficient of friction.
A_f : finial billet area mm^2
R : Extrusion ratio = A_o/A_f
η : Extrusion efficiency.
D : Initial Billet diameter. mm
Y : Average yield stress Kg/mm^2
r : Extrusion reduction $(1 - \frac{1}{R})$
P_1 : Maximum pressure. Kg/mm^2
P_2 : Minimum pressure. Kg/mm^2
v : Axial velocity component. mm/min
u : Radial velocity component. ,,
$\dot{\bar{\epsilon}}$: Equivalent strain rate sec^{-1},
$\bar{\epsilon}$: Equivalent strain .
n : Strain hardening exponent.
K : Strength coefficient . Kg/mm^2
$\bar{\sigma}$: Equivalent stress. ,,
L : Billet length up to the coring point. mm
L_1 : Billet length up to the maximum pressure. ,,
L_2 : Billet length up to the minimum pressure. ,,
V : Average velocity between two points. mm/min.

INTRODUCTION

Extrusion of non circular sections from cylindrical containers has been studied by several workers for different materials and conditions, reported by Jhonson and Kudo[1]. Generally these workers had found that the hole shape for a given reduction influenced the extrusion pressure only slightly. Jhonson[2] studied the flow pattern of square, rectangular, triangular and I-section extrusions and concluded that flow patterns on planes of symmetry were similar to that of plane-strain or axisymmetric extrusions of equivalent sections. The present paper concerns a complete analysis of the effect of the extrusion ratio and the geometery of the extruded section on the total extrusion pressure in terms of the homogeneous, redundant deformation and the frictional work . A modified visioplasticity technique, proposed by Childs[3] and, Farag and Sellars[4], was used to study the flow of metal using split specimens and to calculate equivalent strain, equivalent stress distributions on planes of symmetry of the extruded specimens. Also the value of the redundant deformation was calculated and compared with that obtained from analysing the extrusion pressure.

EXPERIMENTAL WORK

Experimental work was carried out with direct extrusion of non-circular shapes using sharp edged (90°) square dies. Material used was "commercial pure aluminium (99.97%) supplied in form of 40 mm diameter hot extruded rods. Billet dimensions were maintained constant at 30 mm nominal diameter and 40 mm long. The billet was split in half longitudinally prior to extrusion and a grid is applied to one of the split faces. The grid consists of a set of lines parallel to the billet axis, called flow lines,

and a set perpendicular to the first called transverse lines. The two halves of every specimen were anealed for one hour at 350° to produce auniform grain size and were put back together, the billet is partially extruded, removed from the die, separated along the same plane and the grid line distortions are observed. The extrusion experiments were carried out in a sub-press mounted on a 200 ton . Amsler compression testing machine under constant extrusion speed of 7 mm/min. The extrusion container was 30 mm inner diameter. Lubricant used was a suspension of colloidal graphite in acetone and was applied to the billet before extruding, this gives an even film of graphite when acetone had dried off. The method was adopted for all specimens to prevent sticking of both during the extrusion. Eight extrusion ratios of (1.767, 2.5, 3.25, 7.07, 9, 14.14, 28.3 and 36) were used in the present work, and were divided into three sets, every set contained a square, rectangular and circular shapes. At every set the length of the square shape and the width or length of the rectangular shape equals to the diameter of the round shape. Thus, there was three sets of meridian planes, where the flow distortion was examined, passing through the axis of symmetry of the extruded specimens and having an initial dimension equals to the container diameter and exit dimension equals to : 20 mm in the first set, 10 mm in the second set and 5 mm. in the third set. Extrusion experiments were carried out at room temperature.

METHOD OF ANALYSIS

I- EXTRUSION PRESSURE

The extrusion pressure was analysed as Jonas[5], who considered the extrusion pressure to have three components,

a- The homogeneous or ideal work of deformation (P_h).

b- The extra pressure due to the inhomogeneous or redundant deformation (P_r).

c- The pressure required to overcome the sliding resistance to the billet length beyond the dead metal zone due to friction (P_f).

and defined the total extrusion pressure as :

$$P_e = P_h + P_r + P_f \quad \ldots (1)$$

The maximum extrusion pressure obtained experimentally under different extrusion conditions was analysed according to the following procedure :-

1- Ideal extrusion pressure (P_h) . The value of ideal extrusion

pressure was calculated from the relation of

$$P_h = \ln(A_o/A_f) = \ln(R) \quad \ldots (2)$$

and the extrusion efficiency (η) was then defined as

$$\eta = P_h/P_e \quad \ldots (3)$$

2- **Pressure to overcome frictional work (P_f)**

This pressure was estimated according to the suggession of Jonas[6] and Co-workers as

$$P_f = P_e - P_o \quad \ldots (4)$$

and as $$P_e = P_o \exp 4\mu L/D \quad \ldots (5)$$

i.e. $$P_f = P_o \left[\exp(4\mu L/D) - 1 \right]$$

and $P_o = P_h + P_r$ at the coring point.

Therefore the frictional work ratio was taken as (P_f/P_e) .

3- **Pressure required for redundant deformation (P_r)**

Redundant deformation in extrusion arises because of friction along the container walls and the die face, this restraines the free flow of the material resulting in internal shearing in the billet, mainly in a zone that bell shaped in section with the narrowest part of the bell at the die oriffice. The drop in pressure from the start of extrusion to the coring point can be attributed to that required for frictional work. The pressure at the coring point therefore exceeds the pressure for homogeneous deformation by an amount equal to that required for redundant deformation, on this basis the redundant work can be estimated from the following relation

$$P_r = P_o - P_h \quad /\ldots (7)$$

Therefore the redundant work ratio can be calculated as the ratio (P_r/P_e).

DETERMINATION OF THE FLOW STRESS

For a non work-hardening material the yield stress has a constant value but when the material is one of work - hardening materials the yield stress has an increasing value with strain increasing. Johnson[6] suggested an average value of the yield stress $\bar{Y}$ which was defined as the average value of the true stress over the range of logarithmic strain from 0 to $(0.8 + 1.5 \ln \frac{1}{1-r})$, and r, is defined as :

$$r = (1 - A_f/A_o)$$

The flow stress of the material used was considered to be the average yield stress $\bar{Y}$ corressponding to the value of reduction(r).

ESTIMATION OF THE COEFFICIENT OF FRICTION

The apparent coefficient of friction (μ) between the billet material and the container was calculated in the present work from the expression developed by Hirst and Ursel[7]

$$\mu = \frac{D}{4\,(L_2 - L_1)} \ln P_1/P_2 \qquad \ldots \quad (8)$$

Expression (8) is based on the assumption that the drop in extrusion pressure is due intirely to reduced friction between the billet and the container.

II- VISIOPLSTICITY TECHNIQUE

The flow of aluminium under the different extrusion conditions was analysed from measurements of grid lines machined on a meridian plane of partially extruded billets. The measurements are based on the assumption that grid lines initially parallel to the billet axis coincide with the streamlines of the flow and grid lines initially perpendicular to the billet axis represent the progress of deformation at intervals of ram travel equal to the initial grid spacing, i.e. steady state conditions.
The calculations of metal-flow parameters are based on a procedure reported by Childs[3] and modified by Farag and Sellars[4] as follows :
(i) the average velocity V over a length of a streamline between two grid points was taken as proportional to that length and the direction coincides with that portion of streamline. Graphical methods were used to compute the radial and axial components of velocity, u and v, respectively, from V and to smooth their values independently along the streamline.
(ii) the equivalent strain rate $\dot{\bar{\epsilon}}$ was taken as

$$\dot{\bar{\epsilon}} = \sqrt{\frac{2}{3}} \left[\left(\frac{\partial u}{\partial r}\right)^2 + \left(\frac{\partial v}{\partial z}\right)^2 + \left(\frac{u}{r}\right)^2 + \tfrac{1}{2} \left(\frac{\partial u}{\partial z} + \frac{\partial v}{\partial r}\right)^2 \right]^{1/2} \qquad \ldots (9)$$

The values of $\dot{\bar{\epsilon}}$ were calculated at 1.8 mm intervals through out the flow zone. The strain rate components in the above equation were obtained graphically as the slopes of the plotted curves which describe :
1- The variation of v,u independently with r at constant z.
2- The variation of v,u independently with z at constant r.

where r,z are the radial and axial coordinates of the point at which the mean equivalent strain rate was calculated.

(iii) the equivalent strain, $\bar{\epsilon}$, at points on the streamline was calculated from the equivalent strain rate, $\dot{\bar{\epsilon}}$, by integration along the streamlines as the expression represented by Farag and Sellars[4] :

$$\bar{\epsilon} = \int d\bar{\epsilon} = \int \frac{\dot{\bar{\epsilon}}}{v} \, dl \, . \qquad \ldots (10)$$

(iv) Equivalent stress ($\bar{\sigma}$) :- The stress strain curve of many metals in the region of uniform plastic deformation can be expressed by the simple power curve relation[8]

$$\bar{\sigma} = K (\epsilon)^n \qquad \ldots (11)$$

EXPERIMENTAL RESULTS AND DISCUSSION

1- Mechanical behavior of Aluminium :

A compression test was performed on the material used through out the experiments and a true stress-true strain curve was obtained, and it was noticed that the material used is a work-hardening material. Then the material constants in the power curve relation $\bar{\sigma} = k \epsilon^n$, which describe the plastic deformation of the material, was obtained from a log-log plot of the true stress-true strain curve.

The values of the strain hardening exponent, n , and the strength coefficient, k, of the material, were 0.31 and 14.45 kg/mm^2 respectively.

An average yield stress ($\bar{Y}$) was calculated, for different extrusion reductions (r), as the area under the true-true strain curve corresponding to a logarthmic strain ranged between 0,$(0.8 + 1.5 \ln \frac{1}{1-r})$ divided by a value of logarthmic strain of $(0.8 + 1.5 \ln \frac{1}{1-r})$.

- Coefficient of friction : As previonsly illustrated the friction between the container wall and die face plays an important part in determining the pressures required for extrusion and the homogeneity of metal flow. In the present work, the coefficient of friction was calculated during the extrusion experiments and was found to have an average valve of 0.042.

- Extrusion pressure :

Fig.(1) shows that The values of P_h and P_e increased with log (A_o/A_f), but there is a difference between their values due to the inhomogeneous pressure lost in friction and redundant deformation.

The difference between P_e and P_h increased with the increasing of A_o/A_f, because of the increasing of inhomogeneous pressure.
The pressure, P_e , was found to increase with increasing the ratio of length to width for non circular shapes, this is due to the increase in redundant deformation with increase of length to width ratio. It was found that the percent increase of the maximum extrusion pressure for non circular sections over that required for round sections, of the equivalent extrusion ratio, varried between 5-25% for square sections and 13-39% for rectangular sections, of width to length ratio = ½, depending on the extrusion ratio.
Fig.(2) shows that the frictional work ratio P_f/P_e was almost constant, which is understandable since (μ) was constant.
The redundant work ratio, P_r/P_e, Fig. (2) decreased with increasing extrusion ratio (and tended to increase again after extrusion ratio = 14). The decrease in P_r/P_e with the increase in reduction indicates a more homogeneous flow. The redundant work ratio showed a minimum value for all shapes at extrusion ratio = 14. Fig.(2) shows that the square sections had a more homogeneity in flow than rectangular sections of width to length ratio = ½, and the round sections had move homogeneity of flow due to the decrease in redundant value than all other shapes.
The decrease in (P_r/P_e) and its indication of a more homogeneity of flow was reflected in the effeciency of extrusion ($\eta = P_h/P_e$) as shown in Fig.(3) which the extrusion effeciency increased with increasing reduction, due to the improved homogeneity of metal flow caused by the decrease of dead metal volume with increase dead metal zone angle at high reductions. It should be noted that this increase in (η) ,
Fig.(3), tended to decrease again after reduction = 14 this is due to the increase in the value of redundant deformation as discussed previously.
It must be noted that, circular sections had the highest value of extrusion efficiency (η), this is due to the fact that circular sections had a more homogeneous flow than after shapes. It was found that, the extrusion effeciency (η) levels decreased with decreasing the width to length ratio of non circular shapes because of increasing the value of redundant work. It should be noted that, the square shapes had a value of efficiency more than that of rectangular shapes of width to length ratio = ½, which can be attributed to the more homogeneous flow of square shapes than rectangular shapes.

- Flow Patterns and Flow lines :

Fig.(4) shows the photographs of the partly extruded billets, for several shapes and reductions. It should be noted that the distortion of the flow lines was examined on two perpendicular planes for each non-circular section and it was found that the dead metal zone angle measured in a plane passing through the width is more than that found on a plane passing through the length.
The results indicated that the dead metal zone angle increased with decreasing shape thickness along direction of the meridian plane due to the increase in the extrusion ratio.

- Equivalent strain distribution :

The equivalent strain, $\bar{\epsilon}$, was calculated as illustrated previously, using the modified visioplarticity technique. Then the equivalent strain distribution was obtained for various planes of symmetry of different extruded sections at different extrusion ratios.
The amount of redundant deformation involved in extrusion can be evaluated qualitatively by examining the equi-strain contours in the deforming material. The ideal case is when the contours are straight lines at right angles to the billet axis with the highest value equal to $\ln(A_o/A_f)$ where A_o/A_f is the extrusion ratio.
Inspection of the equi-strain contours shown in Fig.(5) shows that the strain values at the die exit are much higher than the ideal value, especially near the extruded bar surface due to the extra shear strains caused by friction.
The amount of redundant deformation was calculated as the difference between the ideal strain, of value equal to $\ln(A_o/A_f)$, and the maximum value of strain obtained in Fig.(5) for every specimen.
Fig.(6) illustrates the variation of such difference (redundant deformation) with the variation of extrusion ratio for different extruded sections, it should be noted that for all sections, the value of redundant deformation decreased with the extrusion ratio increase, till it reaches the extrusion ratio of value 14:1, where a minimum value of redundant deformation was found and then, the redundant deformation tended to increase, again, with the extrusion ratio increase.
Fig.(6) shows that, at the same extrusion ratio, the extruded round section had a value of redundant deformation less than all other shapes, then, the square section had a value of redundant deformation more than that of the round section, but the rectangular section showed the highest values of redundant deformation than round and square sections. It should be noted that the material flow in the square sections is more homogeneous than that of rectangular

Fig.(5) also, shows that, on a plane of symmetry, having the same initial and final dimensions, as the width to length ratio, of a non circular shape, decreases (decreasing the thickness about the plane of symmetry) the value of the redundant deformation decreases also which leads to a more homogeneous deformation in a direction parallel to the length than that which is parallel to the width, which can be attributed to the high resistance to deformation in the width direction.

-Equivalent stress distribution

The equivalent stress distributions was calculated as described before, and the results abtained are shown in Fig.(7) . It should be noted that the value of the stress obtained was directly depending on the values of the strain at these points at which the stress was calculated.

It should be noted that the values of the stress distribution were higher than the yield stress of the material due to the work kardening property of the material used. It was clear that the greatest value of stress was found near the die exit corner because of the resistance to deformation.

The maximum value of the stress increased with increasing of the extrusion ratio.

On a plane of symmetry, having the same initial and final dimensions, the maximum value of stress increased with the decreasing of the width to length ratio of a non-circular shape.

Also, it should be noted that, the maximum value of the stress on a plane of symmetry parallel to the width of a non-circular shape is more than that found on a plane of symmetry parallel to the length, because the resistance to flow in the width direction is more than that in the length direction.

CONCLUSIONS

(1) The rectangular sections required an extrusion pressure more than that required for square sections where the percent increase in pressure, for sections examined over that required for round sections of equivalent extrusion ratio, varried between 5-25% for square sections and 13-39% for rectangular sections depending on the extrusion ratio.

(2) The square sections had a higher value of extrusion efficiency than that of the rectangular sections where the extrusion efficiency was found to be 48% for square sections, 45.8% for rectangular shapes and 51% for round shapes which gave the higher efficiency than all other shapes.

(3) The redundant work ratio was found to have a minimum value at exrusion ratio of 14:1 where the extrusion efficiency was found to be of a maximum value .

(4) Square sections had a more homogeneous than rectangular sections, where the value of redundant strain, measured in square section was found to be less than that found in rectangular sections.

(5) When extruding a rectangular section the flow in a direction parallel to the length is more homogeneous than that in a direction parallel to the width.

(6) The maximum value of the flow stress, near the die exit, on a plane of symmetry parallel to the width of an extruded rectangular section is more than that found on a plane of symmetry parallel to the length.

BIBLIOGRAPHY

1- Johnson, W. and Kudo, H., "The mechanics of metal extrusion", Manchester University press, 1962.

2- Johsnon, W., "Experiments in the cold Extrusion of rods of non circular section", J. Mech. phys. solids, Vol.7, p. 37 (1958) .

3- Childs, T.H.C., "Metals Technology., 1974, L, 305.

4- Farag, M.M., Sellars, C.M., Analysis of double maximum flow patterns in axisymmetric extrusion of HH 30 Aluminium alloy, Metals Technology May 1975, p. 220.

5- Jonas, J.J., McQueen, H.J., and Wong, W.A., "Derformation under hot working conditions." I.S.I. Special Report, No.108, p. 49, (1968).

6- Jhonson, W., Mellor, P.B. "Plasticity for Mechanical Engineers" Van Nostrand (1962).

7- Hirst, S. And Ursell, D.H., "Metal treatment, 25, 409, (1958).

8- Dieter, George, E., Mechanical Mitallargy, Mc. Graw-Hill, Kogakusha. 1961.

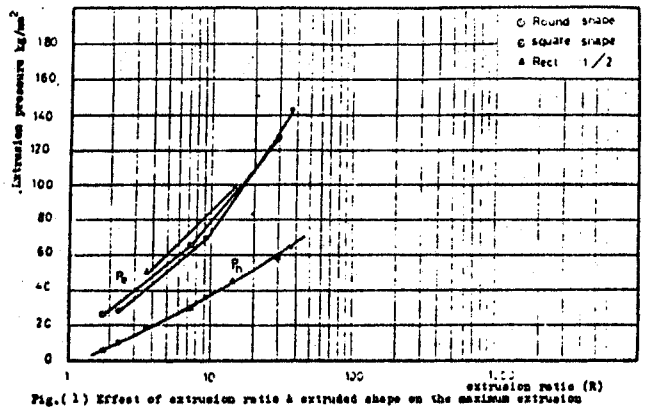

Fig.(1) Effect of extrusion ratio & extruded shape on the maximum extrusion pressure P_e and on the homogeneous pressure P_h.

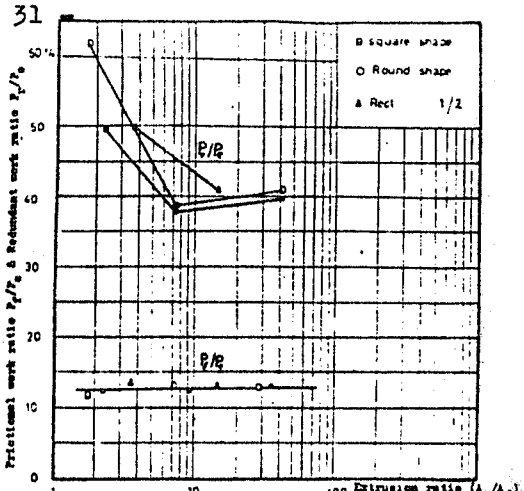

Fig.(2) Effect of extrusion ratio (A_o/A_f) & extruded shape on the redundent work ratio P_r/P_e and frictional work ratio P_f/P_e

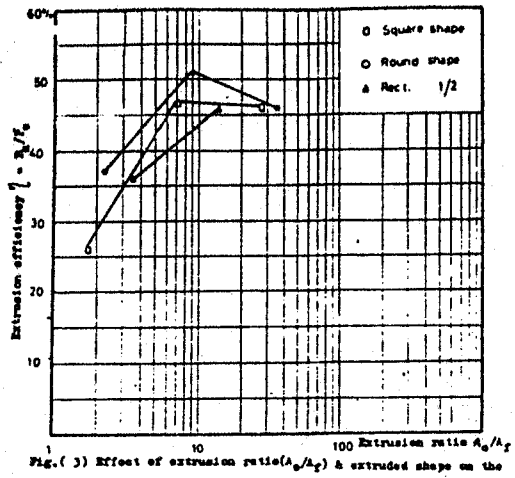

Fig.(3) Effect of extrusion ratio(A_o/A_f) & extruded shape on the extrusion efficiency $= P_h/P_e$.

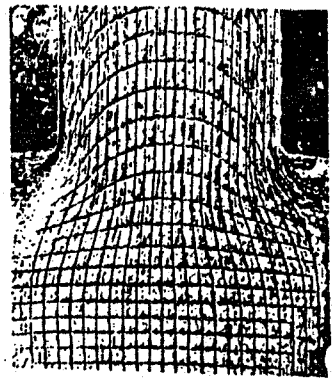

Fig.(4-1) Flow pattern & deformation of grid lines on a split billet in a meridian plane of a square extruded section 20 x 20 mm.

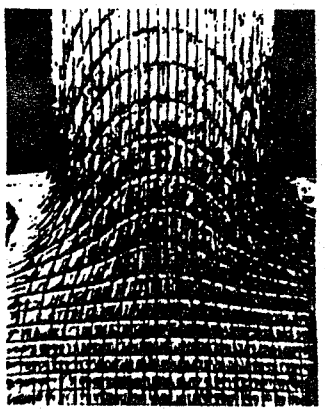

Fig.(4-2) Flow pattern & deformation of grid lines on a split billet in a meridian plane of a round extruded section 20$^{\phi}$ mm.

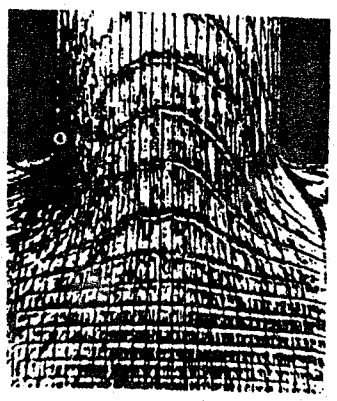

Fig.(4-3) Flow pattern & deformation of grid lines on a split billet in a meridian plane parallel to the length of a rectangular extruded section 20 x 10 mm

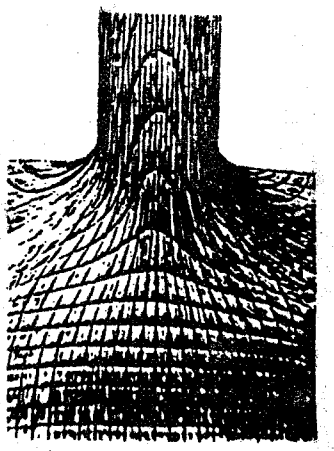

Fig.(4-4) Flow pattern & deformation of grid lines on a split billet in a meridian plane parallel to the width of a rectangular extruded section 20 x 10 mm.

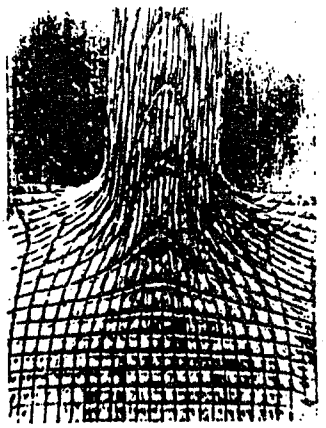

ig.(4-5) Flow pattern & deformation of grid lines on a split billet in a meridien plane of a square extruded section 10 x 10 mm.

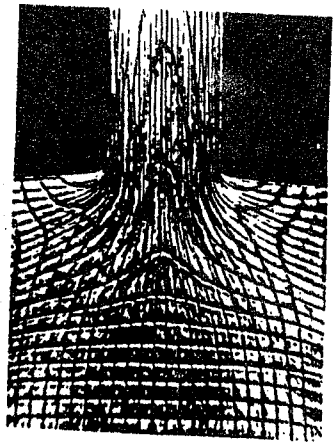

Fig.(4-6) Flow pattern & deformation of grid lines on a split billet in a meridien plane of a round extruded section 10^{ϕ} mm.

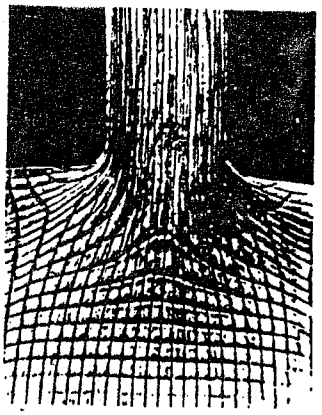

Fig.(4-7) Flow pattern & deformation of grid lines on a split billet in a meridien plane parallel to the length of a rectangular extruded section 10 x 5 mm.

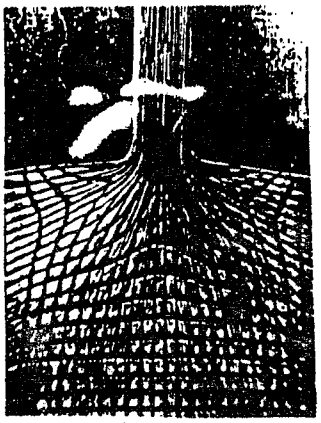

ig.(4-8) Flow pattern & deformation of grid lines on a split billet in a meridien plane parallel to the width of a rectangular extruded section 10 x 5 mm.

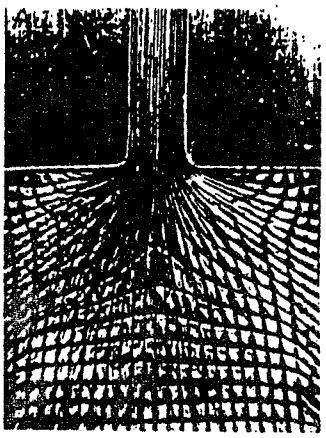

Fig.(4-9) Flow pattern & deformation of grid lines on split billet in a meridien plane of a square extruded section 5 x 5 mm.

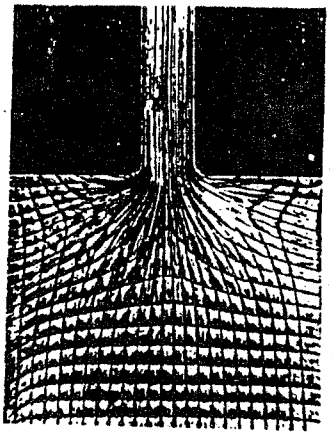

Fig.(4-10) Flow pattern & deformation of grid lines on a split billet in a meridien plane of a round extruded section 5^{ϕ} mm.

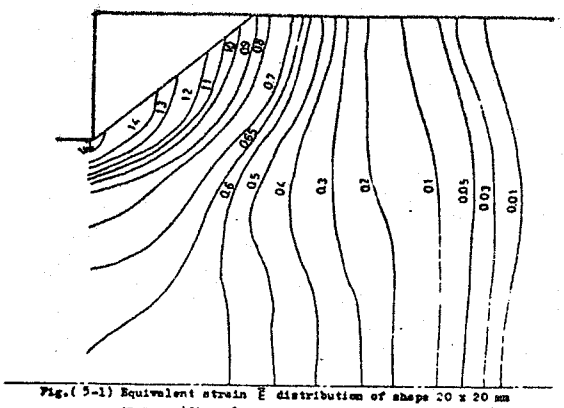

Fig.(5-1) Equivalent strain $\bar{\varepsilon}$ distribution of shape 20 x 20 mm on a meridian plane.

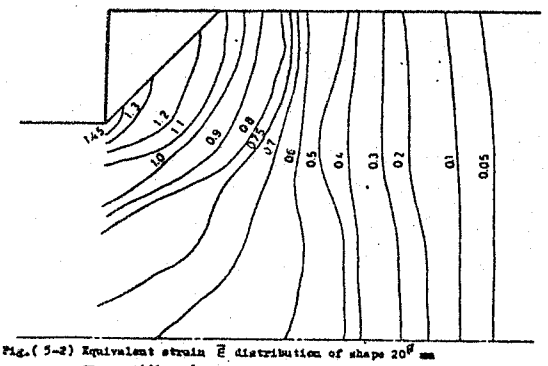

Fig.(5-2) Equivalent strain $\bar{\varepsilon}$ distribution of shape 20^{ϕ} mm on a meridian plane.

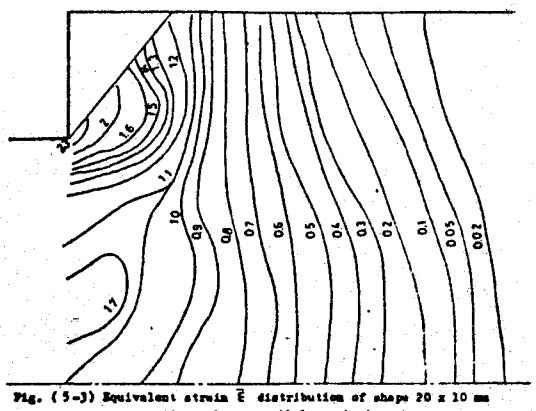

Fig. (5-3) Equivalent strain $\bar{\varepsilon}$ distribution of shape 20 x 10 mm on a meridian plane parallel to the length.

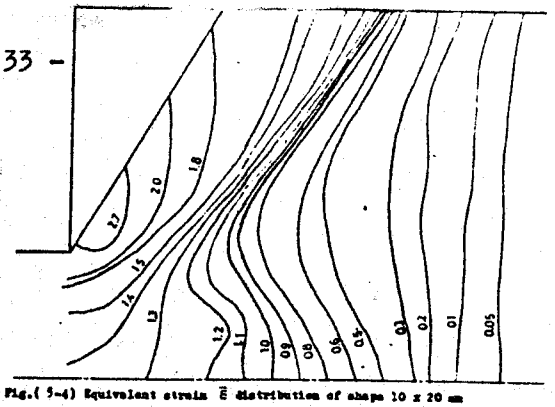

Fig.(5-4) Equivalent strain $\bar{\varepsilon}$ distribution of shape 10 x 20 mm on a meridian plane parallel to the width.

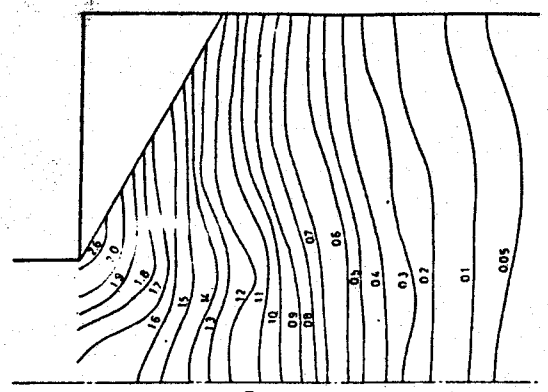

Fig.(5-5) Equivalent strain $\bar{\varepsilon}$ distribution of shape 10 x 10 mm on a meridian plane.

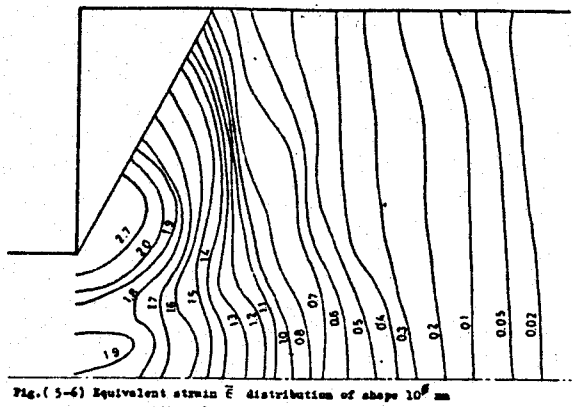

Fig.(5-6) Equivalent strain $\bar{\varepsilon}$ distribution of shape $10^{\#}$ mm on a meridian plane.

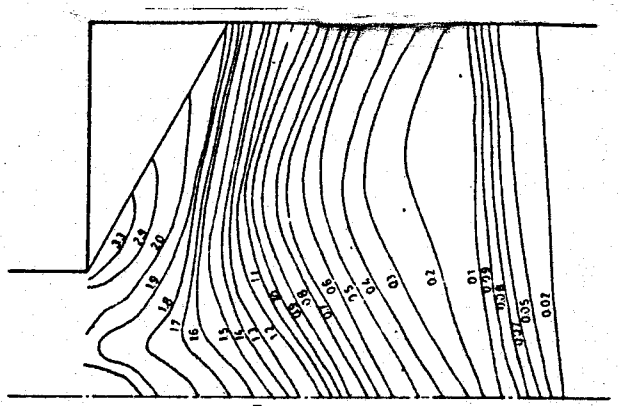

Fig.(5-7) Equivalent strain $\bar{\varepsilon}$ distribution of shape 5 x 10 mm on a meridian plane parallel to the length.

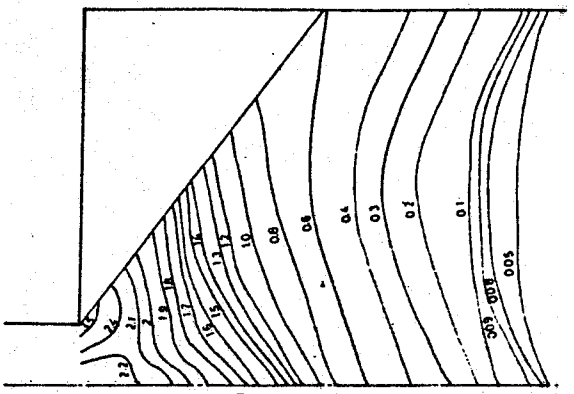

Fig.(5-8) Equivalent strain $\bar{\varepsilon}$ distribution of shape 5 x 10 mm on a meridian plane parallel to the width.

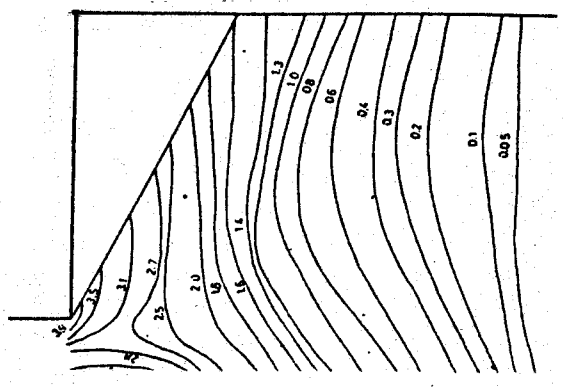

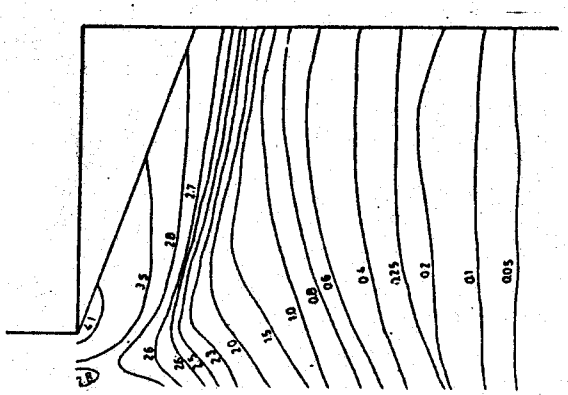

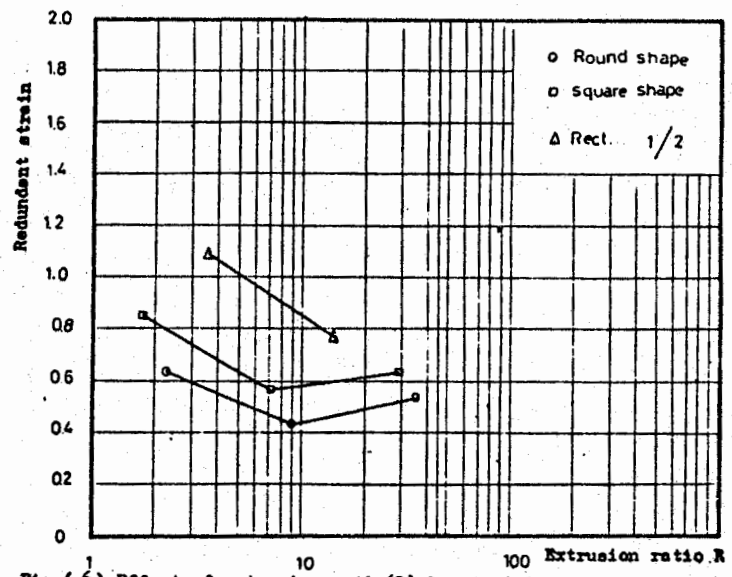

Fig.(6) Effect of extrusion ratio(R) & extruded shape on the redundant strain.

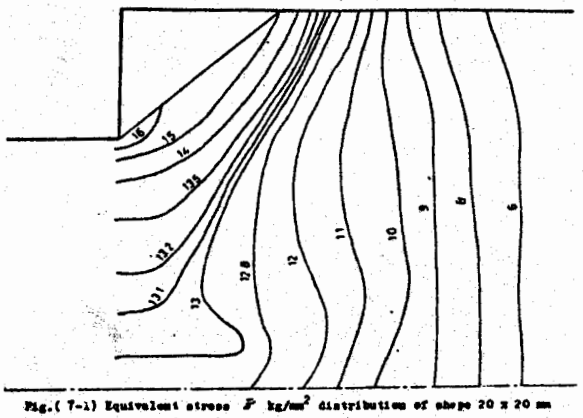

Fig.(7-1) Equivalent stress $\bar{\sigma}$ kg/mm^2 distribution of shape 20 x 20 mm on a meridian plane.

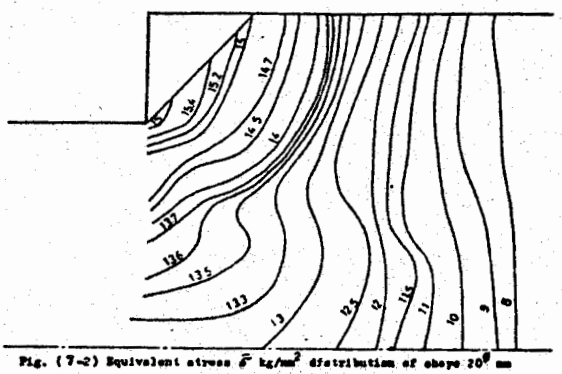

Fig. (7-2) Equivalent stress $\bar{\sigma}$ kg/mm^2 distribution of shape 20$^{\phi}$ mm on a meridian plane.

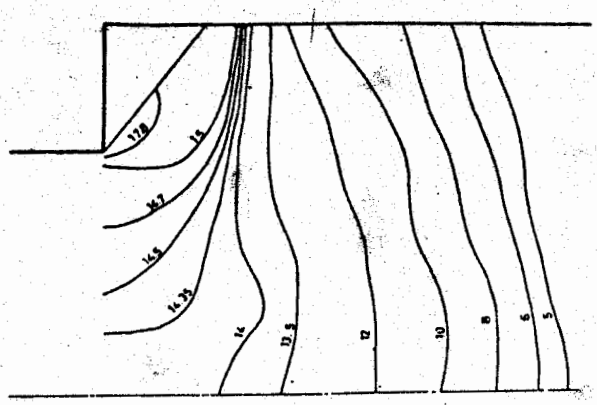

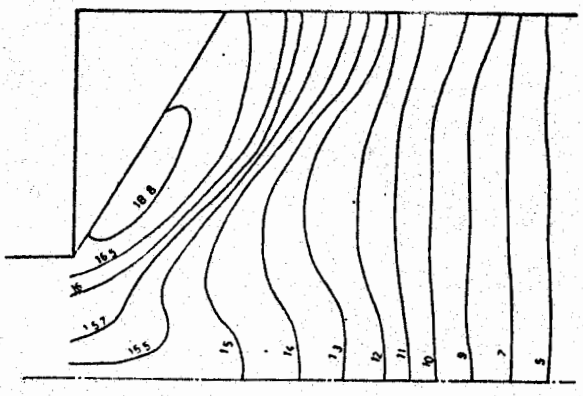

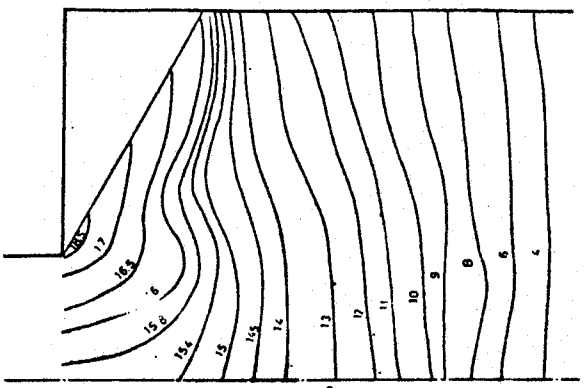

Fig.(7-5) The equivalent stress $\bar{\sigma}$ kg/mm^2 distribution of shape 10 x 10 mm on a meridian plane.

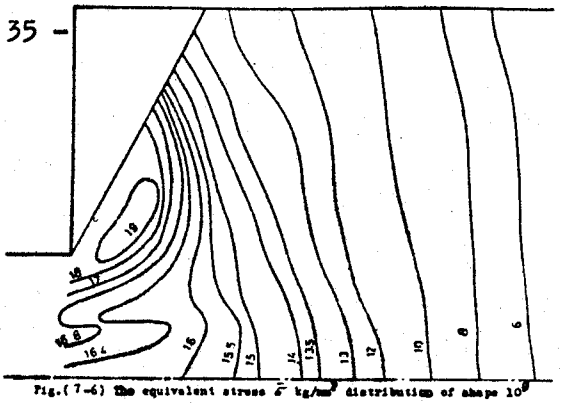

Fig.(7-6) The equivalent stress $\bar{\sigma}$ kg/mm^2 distribution of shape 10 on a meridian plane.

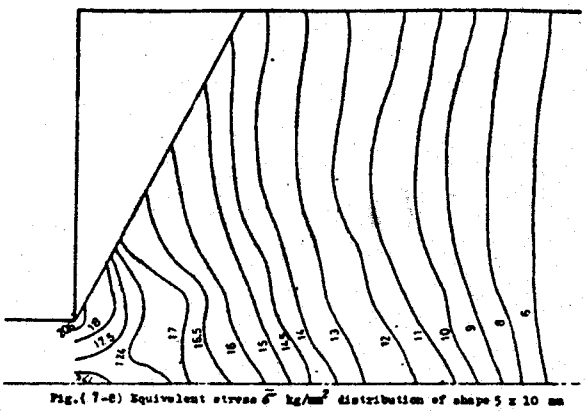

Fig.(7-8) Equivalent stress $\bar{\sigma}$ kg/mm^2 distribution of shape 5 x 10 mm on a meridian plane parallel to the width.

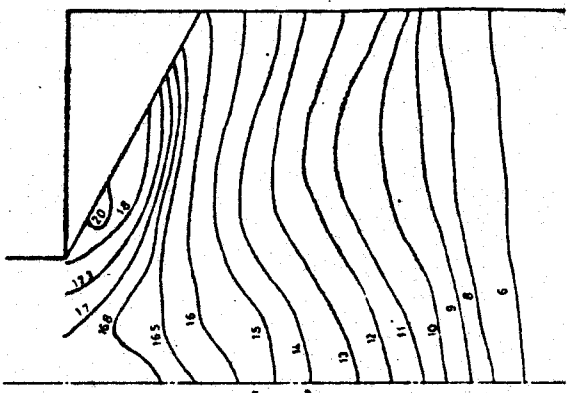

Fig.(7-7) Equivalent stress $\bar{\sigma}$ kg/mm^2 distribution of shape 10 x 5 mm on a meridian plane parallel to the length.

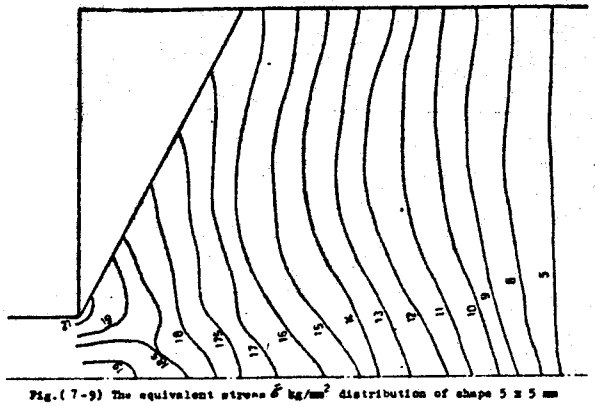

Fig.(7-9) The equivalent stress $\bar{\sigma}$ kg/mm^2 distribution of shape 5 x 5 mm on a meridian plane.

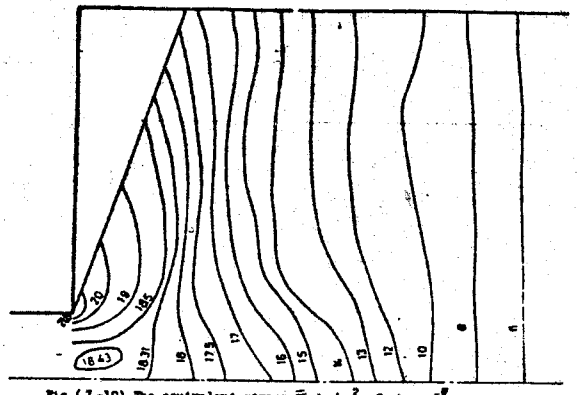

Fig.(7-10) The equivalent stress $\bar{\sigma}$ kg/mm^2 of shape 5 on a meridian plane.